

NON-CLASSICAL PROPERTIES AND GENERATION SCHEMES OF SUPERPOSITION OF MULTIPLE-PHOTON-ADDED TWO-MODE SQUEEZED VACUUM STATE

Tran Quang Dat ^{1,2}, Truong Minh Thang¹, Truong Minh Duc^{1*}

¹Department of Physics, University of Education, Hue University, 34 Le Loi St., Hue, Vietnam

²University of Transport and Communications, 3 Cau Giay St., Dong Da Dist., Hanoi, Vietnam

* Correspondence to Truong Minh Duc <tmduc2009@gmail.com>

(Received: 7 October 2020; Accepted: 31 October 2020)

Abstract. In this paper, we study some non-classical properties and propose the generation schemes of the superposition of multiple-photon-added two-mode squeezed vacuum state (SMPA-TMSVS). Based on the Wigner function, we clarify that this state is a non-Gaussian state, while the original two-mode squeezed vacuum state (TMSVS) is a Gaussian state. Besides, the SMPA-TMSVS is sum squeezing, as well as difference squeezing. In particular, the manifestation of the sum squeezing and the difference squeezing in the SMPA-TMSVS becomes more pronounced when increasing parameters r and ϵ . In addition, by exploiting the schemes of photon-added superposition in the usual order, we give some schemes that the SMPA-TMSVS can be generated with the higher-order photon-added superposition by using some optical devices.

Keywords: Photon-added two-mode squeezed vacuum state, Wigner function, sum squeezing, difference squeezing, generation scheme

1 Introduction

Non-classicality of non-classical states plays a central role in the quantum tasks such as detecting gravitational waves via the LIGO interferometer by using squeezing light [1], producing single-photon resources by exploiting the anti-bunching effect [2], and implementing protocols in the quantum information by applying entangled sources [3, 4]. To improve the effectiveness of these tasks, researchers have studied the methods that can enhance the degree of non-classicality of the non-classical states [5-8]. The primary method is the photon addition operation to any states, including coherent states [5, 9-12] and squeezed states [13-15].

We know that the local photon addition operation to multimode states changes classical states to non-classical states [16] and increases the manifestation of squeezing and entanglement in original non-classical states [6, 8, 12, 15, 17]. However, in the weak region of the amplitude of these states, the role of photon addition operation becomes fainter [7, 12]. Therefore, the nonlocal photon addition operation was soon studied [18-20]. This operation can generate maximally entangled states, e.g., the NOON states [18, 19], even though the input fields are vacuum states [18-20].

We pay attention to the two-mode squeezed vacuum state (TMSVS) in the two-mode continuous variables regime [21]. This state is a Gaussian state with a high degree of non-

classicality when the squeezed amplitude is large. Therefore, it is suitable to implement quantum tasks such as quantum teleportation [3], quantum cryptography, quantum dense code, and quantum error correction [22]. Interestingly, this state was generated in the laboratory to perform the quantum teleportation process [23]. However, the amplitude of the generated state is small. For that reason, we are interested in studying the nonlocal photon addition operation on the TMSVS to enhance the quantum effects of the proposed state. Recently, the multiple-photon-added two-mode squeezed vacuum state (SMPA-TMSVS) was introduced in [24] by performing the addition of the superposition of operators a^{+h} and b^{+k} to a TMSVS where a^+ and b^+ are the boson creation operations, and h and k are nonnegative integers. In this state, the degree of entanglement, EPR correlation, quantum steering, and the quantum teleportation process via the SMPA-TMSVS are studied.

In this paper, we present the investigation of the non-classicality of the SMPA-TMSVS. In Section 2, we study the Wigner function of the SMPA-TMSVS. The sum squeezing and the difference squeezing of such a state are examined in detail in Sections 3 and 4. We also propose the experimental schemes for generating this state with some specific values of h and k in Section 5. Finally, we briefly summarize the main results of the paper in the conclusions.

$$A_{h,k}^{p,q,m,l}(r) = \langle r, h, k | a^p a^{+q} b^m b^{+l} | r, h, k \rangle \\ = N_{h,k}^2(r) [N_{p+h,q+h,m,l}(r) + \varepsilon^2 N_{p,q,m+k,l+k}(r) + \varepsilon N_{p+h,q,m,l+k}(r) + \varepsilon N_{p,q+h,m+k,l}(r)],$$

where p, q, m, l are also nonnegative integers.

2 Wigner function

In terms of the Fock states, the TMSVS state [21] is given by

$$|r\rangle_{ab} = \cosh^{-1} r \sum_{n=0}^{\infty} \tanh^n r |n, n\rangle_{ab}, \quad (1)$$

where $|n, n\rangle_{ab} = |n\rangle_a |n\rangle_b$ is a normal product of two Fock states corresponding to two modes a and b , and the squeezed parameter r is real. From the TMSVS given in Eq. (1), the SMPA-TMSVS was recently defined in the form as [24]

$$|r; h, k\rangle_{ab} = N_{h,k}(r) (a^{+h} + \varepsilon b^{+k}) |r\rangle_{ab}, \quad (2)$$

where the normalized coefficient $N_{h,k}$ is determined by

$$N_{h,k}^{-2}(r) = h! \cosh^{2h} r + \varepsilon^2 k! \cosh^{2k} r. \quad (3)$$

In terms of the two-mode Fock states, the SMPA-TMSVS in Eq. (2) is written as

$$|r, h, k\rangle_{ab} = \sum_{n=0}^{\infty} \sum_{i=0}^1 c_{n,i}(r) |n+h_i, n+k_i\rangle_{ab}, \quad (4)$$

therein

$$c_{n,i}(r) = N_{h,k}(r) \cosh^{-1} r \frac{\varepsilon^i \sqrt{(n+h_i)!(n+k_i)!} \tanh^n r}{n!}, \quad (5)$$

where $h_0 = h, h_1 = 0, k_0 = 0, k_1 = k$. In addition, by setting

$$N_{x,y,u,v}(r) = {}_{ba} \langle r | a^x a^{+y} b^u b^{+v} | r \rangle_{ab} = \sum_{n=0}^{\min[x,u]} \frac{x! y! u! v! \cosh^{2x+2u} r \sinh^{v-u}(2r) \tanh^{2n} r \delta_{x+v, y+u}}{2^{v-u} n! (x-n)! (u-n)! (v-u+n)!}, \quad (6)$$

where x, y, u, v are nonnegative integers, and δ is denoted as the Kronecker delta function; the quantum average of operators $a^p a^{+q} b^m b^{+l}$ in the SMPA-TMSVS is given as

The Wigner function is a quasi-probability used to describe the quantum state in the phase space. The negativity of the Wigner function is a witness of non-classicality and non-Gaussian

$$W = \frac{4e^{2(|\alpha_a|^2 + |\alpha_b|^2)}}{\pi^4} \int d^2\gamma_a d^2\gamma_b e^{2(\gamma_a^* \alpha_a + \gamma_b^* \alpha_b - \gamma_a \alpha_a^* - \gamma_b \alpha_b^*)} {}_{ba} \langle -\gamma_b, -\gamma_a | \rho_{ab} | \gamma_a, \gamma_b \rangle_{ab}, \quad (8)$$

where α_a and α_b receive the complex values, and $|\gamma_a, \gamma_b\rangle_{ab} = |\gamma_a\rangle_a |\gamma_b\rangle_b$ denotes a two-mode coherent state. We use Eq. (8) to calculate the Wigner function of the SMPA-TMSVS. With the term of this state given in Eq. (4), the density operator of the SMPA-TMSVS is written as

$$W = \frac{4}{\pi^2} \sum_{m,n=0}^{\infty} \sum_{i,j=0}^1 c_{n,i}(r) c_{m,j}(r) e^{-2(|\alpha_a|^2 + |\alpha_b|^2)} \frac{(2\alpha_a^*)^{n+h_i} (2\alpha_a)^{m+h_j} (2\alpha_b^*)^{n+k_i} (2\alpha_b)^{m+k_j}}{\sqrt{(n+h_i)!(n+k_i)!(m+h_j)!(m+k_j)!}} \times {}_2F_0\left(-n-h_i, -m-h_j; -\frac{1}{|\alpha_a|^2}\right) {}_2F_0\left(-n-k_i, -m-k_j; -\frac{1}{|\alpha_b|^2}\right), \quad (10)$$

where ${}_2F_0$ denotes the hypergeometric function.

We use the analytical expression in Eq. (10) to investigate the non-Gaussian and non-classical characteristics in the SMPATMSVS. In Fig. 1, we plot the dependence of the Wigner function on r when $\alpha = \beta = 0.01$, and $\varepsilon = 1$ for several values of h and k . The results show in the SMPA-TMSVS that the Wigner function can take negative values in some regions of r . Moreover, in some points of the phase space, as the values of r (h, k) increase, the negativity of the Wigner function can increase. This proves that the SMPA-TMSVS is a non-Gaussian as well as a non-classical state.

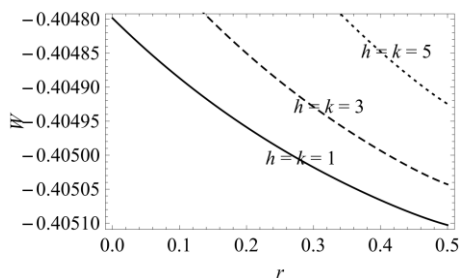


Fig. 1. Wigner function (W) as a function of r when $\alpha = \beta = 0.01$ and $\varepsilon = 1$ for $h = k = 1$ (the solid line), $h = k = 3$ (the dash curve), and $h = k = 5$ (the dotted curve)

characteristics of a non-classical state [25]. In the two-mode continuous variables regime, the Wigner function of a state with a density operator ρ is given in terms of the coherent states as

$$\rho_{ab} = |r, h, k\rangle_{ab} \langle r, h, k| = \sum_{m,n=0}^{\infty} \sum_{i,j=0}^1 c_{n,i}(r) c_{m,j}(r) |n+h_i, n+k_i\rangle_{ab} \langle m+h_j, m+k_j|. \quad (9)$$

According to the calculation method shown in [12], the Wigner function of the SMPA-TMSVS is determined as

3 Sum squeezing

The squeezing property plays an essential role in high-accuracy experiments, such as detecting gravitational waves [1] and cooling materials [26]. The sum squeezing property is associated with the creation of light with the sum frequency at the output. The sum squeezing criterion was first introduced by Hillery [27]. Then, it was applied to detect squeezing in several states [6, 7]. To imagine this criterion, for two arbitrary modes a and b , we consider an operator in the form

$$V_\phi = \frac{1}{2} (e^{i\phi} a^+ b^+ + e^{-i\phi} ab), \quad (11)$$

where ϕ is real. A sum squeezing factor is defined as

$$S = \frac{4 \langle (\Delta V_\phi)^2 \rangle - \langle N_a + N_b + 1 \rangle}{\langle N_a + N_b + 1 \rangle}, \quad (12)$$

where $\langle (\Delta V_\phi)^2 \rangle = \langle V_\phi^2 \rangle - \langle V_\phi \rangle^2$ and $N_x = x^+ x$, $x = \{a, b\}$. A state is called a sum squeezing if it satisfies $S <$

0. Factor S also manifests the squeezing degree, i.e., the more negative S gets, the higher the squeezing degree receives. The sum squeezing

$$S = \frac{2 \cos(2\varphi) \langle a^2 b^2 \rangle - 4 \cos^2 \varphi \langle ab \rangle^2 + 2 \langle aa^+ bb^+ \rangle - 2 \langle aa^+ \rangle - 2 \langle bb^+ \rangle + 2}{\langle aa^+ \rangle + \langle bb^+ \rangle - 1}. \quad (13)$$

Using Eq. (7), we obtain

$$S = \frac{2 \cos(2\varphi) A_{h,k}^{2,0,2,0}(r) - 4 \cos^2 \varphi \left(A_{h,k}^{1,0,1,0}(r) \right)^2 + 2 A_{h,k}^{1,1,1,1}(r) - 2 A_{h,k}^{1,1,0,0}(r) - 2 A_{h,k}^{0,0,1,1}(r) + 2}{A_{h,k}^{1,1,0,0}(r) + A_{h,k}^{0,0,1,1}(r) - 1}. \quad (14)$$

We use the analytical expression in Eq. (14) to clarify the sum squeezing property in the SMPA-TMSVS. In our calculations, the sum squeezing factor is almost unchanged when increasing h , k , and ε . For example, if $\phi = \pi/2$, $r = 2$, with any values of ε , h , k , we only obtain $S \approx -0.96$. However, factor S varies with ϕ . In Fig. 2, we plot the dependence of sum squeezing factor S on r for several values of ϕ . The results show that the degree of sum squeezing gets a maximum at $\phi =$

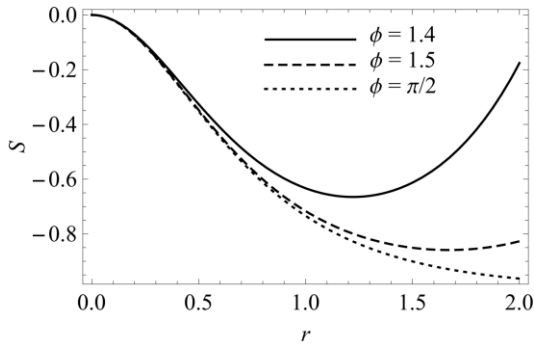


Fig. 2. Sum squeezing factor (S) as a function of r when $\phi = 1.4$ (the solid line), $\phi = 1.5$ (the dashed curve), and $\phi = \pi/2$ (the dotted curve)

$$D = \frac{2 \cos(2\varphi) \langle a^+ b^2 \rangle - 4 \cos^2 \varphi \langle a^+ b \rangle^2 + 2 \langle aa^+ bb^+ \rangle - \langle aa^+ \rangle - \langle bb^+ \rangle - |\langle aa^+ \rangle - \langle bb^+ \rangle|}{|\langle aa^+ \rangle - \langle bb^+ \rangle|}. \quad (17)$$

Using Eq. (7), we write the difference squeezing factor as

$$D = \frac{2 \cos(2\varphi) A_{h,k}^{0,2,2,0}(r) - 4 \cos^2 \varphi \left(A_{h,k}^{0,1,1,0}(r) \right)^2 + 2 A_{h,k}^{1,1,1,1}(r) - A_{h,k}^{1,1,0,0}(r) - A_{h,k}^{0,0,1,1}(r) - |A_{h,k}^{1,1,0,0}(r) - A_{h,k}^{0,0,1,1}(r)|}{|A_{h,k}^{1,1,0,0}(r) - A_{h,k}^{0,0,1,1}(r)|}. \quad (18)$$

factor in the SMPATMSVS is given in the explicit form as

$\pi/2$ (generalized as $\phi = (2m + 1)\pi/2$ with integer m). In this case, factor S becomes more and more negative when parameter r is getting bigger and bigger.

4 Difference squeezing

The difference squeezing criterion was also proposed by Hillery [27]. Accordingly, let us consider another two-mode operator as

$$X_\varphi = \frac{1}{2} (e^{i\varphi} ab^+ + e^{-i\varphi} a^+ b), \quad (15)$$

The two-mode difference squeezing factor is determined as

$$D = \frac{4 \langle (\Delta X_\varphi)^2 \rangle - |\langle N_a - N_b \rangle|}{|\langle N_a - N_b \rangle|}. \quad (16)$$

A state is called a difference squeezing if $D < 0$. This condition was verified in the two-mode photon-added displaced squeezed states [6]. In the SMPA-TMSVS, the difference squeezing factor becomes.

We use the analytical expression in Eq. (18) to examine the difference squeezing behavior in the SMPA-TMSVS. In our numerical calculation, the difference squeezing only appears in the case of single-photon adding $h = k = 1$. For example, when $\epsilon = 0.5$, $\phi = 0$, $r = 0.1$ and $h = k = 1$ (2, 3, 4), we get $D = -0.24$ (2.28, 0.89, 0.92). Besides, in Fig. 3, we plot the dependence of difference squeezing factor D on r when $\phi = 0$, $h = k = 1$ for several values of ϵ . The results show that the degree of difference squeezing enhances when ϵ increases. However, the negativity of factor D increases when r becomes bigger. In addition, we note that the degree of difference squeezing achieves a maximum when $\epsilon = m\pi$ with integer m (see Fig. 4). It should be noted that the original TMSVS does not exist the difference squeezing. Therefore, the photon-added superposition operation on the TMSVS plays an important role to emerge the difference squeezing in the proposed state.

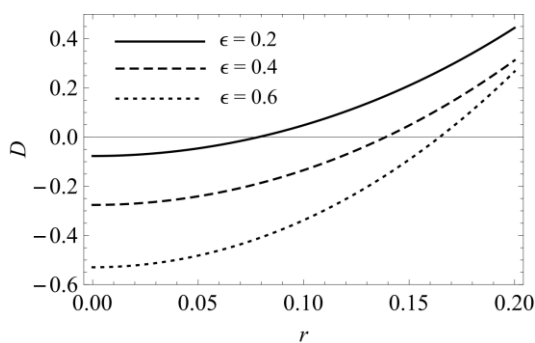


Fig. 3. Difference squeezing factor (D) as a function of r when $\phi = 0$ and $h = k = 1$ for $\epsilon = 0.2$ (the solid line), $\epsilon = 0.4$ (the dashed curve), and $\epsilon = 0.6$ (the dotted curve)

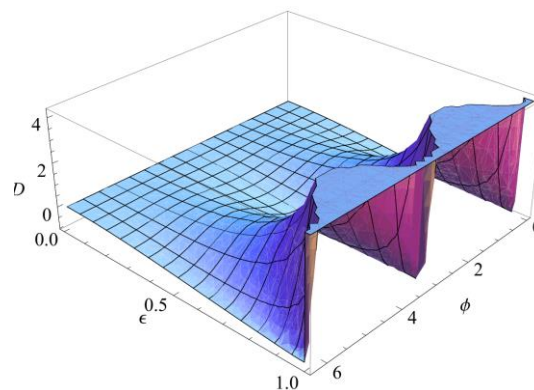


Fig. 4. Difference squeezing factor (D) as a function of ϕ and ϵ when $h = k = 1$ and $r = 0.01$

5 Generation schemes

In order to generate the SMPA-TMSVS with the superposition of photon addition in the usual order and second order as $a^+ + \epsilon b^+$ and $a^{2+} + \epsilon b^{2+}$, several experimental schemes have been proposed [18, 19]. When $h = k > 2$, using the scheme to generate the superposition $xa^+ + yb^+$ of Fiurasek [18], we apply this operation on the TMSVS h times. In each repetition, the values for x and y need to be changed accordingly. For example, the protocol is sketched in Fig. 5 when $h = k = 3$. In this scheme, the values of x_1, y_1, x_2, y_2 are adjusted as

$$\begin{cases} x_1x_2y + xx_1y_2 + xx_2y_1 = 0 \\ xy_1y_2 + x_1yy_2 + x_2yy_1 = 0. \end{cases} \quad (19)$$

Therefore, at the output, the action of the superposition is written as

$$\begin{aligned} &(x_2a^+ + y_2b^+)(x_1a^+ + y_1b^+)(xa^+ + yb^+) |r\rangle_{ab} \\ &= (xx_1x_2a^{+3} + yy_1y_2b^{+3}) |r\rangle_{ab}. \end{aligned} \quad (20)$$

By setting $\epsilon = yy_1y_2/xx_1x_2$, the state in Eq. (20) returns to the SMPATMSVS when $h = k = 3$.

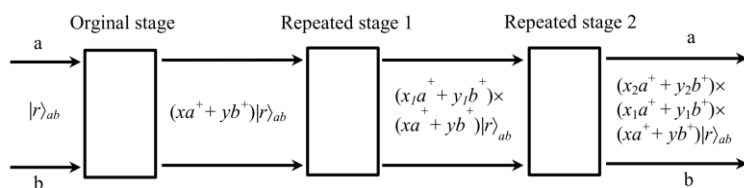


Fig. 5. Experimental scheme generates the SMPATMSVS when $h = k = 3$

Note: The input is a TMSVS $|r\rangle_{ab}$ with two modes a and b . Each rectangle plays the role of performing a usual-order photon-added superposition.

When $h \neq k$, we propose a scheme for generating the SMPA-TMSVS when $h = 1, k = 2$ by using some optical devices. Specifically, the scheme uses a parametric down-converter (PDC) with very weak intensity, a third-order nonlinear crystal (TONC), a balanced beam splitter (BS), and two photo-detectors (PDs). Also, in this scheme, we use a TMSVS and two vacuum states at inputs. The arrangement of these physical resources is depicted in Fig. 6.

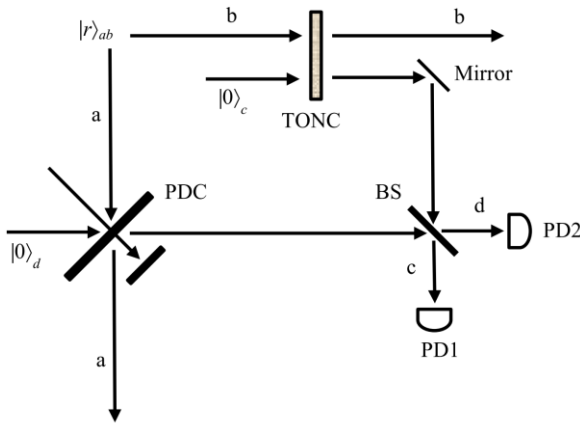


Fig. 6. Experimental scheme generating a SMPATMSVS when $h = 1, k = 2$

Note: The inputs include a TMSVS $|r\rangle_{ab}$ of two modes a and b , and two vacuum states $|0\rangle_c$ and $|0\rangle_d$, corresponding to two modes c and d . PDC is a parametric down-converter. TONC is a third-order nonlinear crystal. BS is a balanced beam splitter. The two modes c and d are detected by two photo-detectors PD1 and PD2, respectively.

$$\begin{aligned}
 |\psi_1\rangle_{abcd} &\approx \left[1 - \frac{\kappa b^{+2} c^+ + d^+}{\sqrt{2}}\right] \left[1 - \frac{\lambda a^+ (-c^+ + d^+)}{\sqrt{2}}\right] |r\rangle_{ab} |0\rangle_c |0\rangle_d \\
 &= \left[1 - \frac{\kappa b^{+2} c^+ + \kappa b^{+2} d^+}{\sqrt{2}} - \frac{-\lambda a^+ c^+ + \lambda a^+ d^+}{\sqrt{2}} + \frac{\kappa b^{+2} \lambda a^+ (c^+ + d^+) (-c^+ + d^+)}{2}\right] |r\rangle_{ab} |0\rangle_c |0\rangle_d \\
 &= \left[1 - \frac{(\kappa b^{+2} - \lambda a^+) c^+}{\sqrt{2}} - \frac{(\kappa b^{+2} + \lambda a^+) d^+}{\sqrt{2}} + \frac{\kappa b^{+2} \lambda a^+ (c^+ + d^+) (-c^+ + d^+)}{2}\right] |r\rangle_{ab} |0\rangle_c |0\rangle_d.
 \end{aligned} \tag{25}$$

Now, if the photo-detectors PD1 and PD2 detect 0 (1) and 1 (0) photons in modes c and d , respectively, the output state is arranged in the term

$$|\psi_{out}\rangle_{ab} = \left(\frac{-\kappa}{\sqrt{2}} b^{+2} + \frac{\lambda}{\sqrt{2}} a^+\right) |r\rangle_{ab}, \tag{26}$$

The action of the PDC is characterized by the operator

$$s(\lambda) = e^{-\lambda a^+ d^+ + \lambda^* a d}, \tag{21}$$

where λ is the coupling strength of the PDC, $\lambda \ll 1$. On the other hand, the transformation of the TONC is described by

$$K(\kappa) = e^{-\kappa b^{+2} c^+ + \kappa^* b^2 c}, \tag{22}$$

where κ is proportional to the third-order nonlinearity of the TONC. Besides, with the BS 50:50, the input fields corresponding to operator c and d are changed into $(c+d)/\sqrt{2}$ and $(-c+d)/\sqrt{2}$ at the outputs, respectively.

The state of the system after simultaneously passing through the PDC and the TONC is

$$|\psi\rangle_{abcd} = e^{-\kappa b^{+2} c^+ + \kappa^* b^2 c} e^{-\lambda a^+ d^+ + \lambda^* a d} |r\rangle_{ab} |0\rangle_c |0\rangle_d. \tag{23}$$

If the intensity of the PDC and the TONC is very weak, the state in Eq. (23) approximates

$$|\psi\rangle_{abcd} \approx (1 - \kappa b^{+2} c^+) (1 - \lambda a^+ d^+) |r\rangle_{ab} |0\rangle_c |0\rangle_d. \tag{24}$$

Next, after mode c and d are driven simultaneously to the BS, the state $|\psi\rangle_{abcd}$ becomes

or

$$|\psi_{out}\rangle_{ab} = \left(\frac{-\kappa}{\sqrt{2}} b^{+2} - \frac{\lambda}{\sqrt{2}} a^+\right) |r\rangle_{ab}. \tag{27}$$

By setting $\varepsilon = -\kappa/\lambda$ (κ/λ), the state in Eq. (26) or (27) returns to the SMPA-TMSVS when $h = 1, k = 2$. It should be noted that we can use the above

scheme for multiple times to generate the SMPA-TMSVS if $h > 1$ and $k > 2$.

6 Conclusions

In this paper, we investigate the Wigner function, the sum squeezing, and the difference squeezing in the SMPA-TMSVS. Considering the negativity of the Wigner function, we show that due to the addition of the photons to the two modes of a TMSVS, the SMPA-TMSVS state becomes a non-Gaussian state, whereas the original TMSVS is the Gaussian state. Besides, the SMPA-TMSVS is the sum squeezing, and the degree of sum squeezing enhances by increasing the squeezed parameter r instead of changing parameters h , k , and ε . In contrast to the TMSVS, the SMPA-TMSVS is the difference squeezing, and the squeezing degree is improved by raising ε . This demonstrates the importance of the photon-added superposition operation to the original TMSVS. More importantly, we clarify that the SMPA-TMSVS can be generated by using the scheme of Fiurasek multiple times when $h = k > 2$. In addition, using some optical devices like PDC, TONC, BS, and PDs, we have proposed an experimental scheme to generate an SMPA-TMSVS if $h = 1$ and $k = 2$. Combining this scheme with that of Fiurasek, Lee and Nha, it is possible to generate the SMPA-TMSVS with a higher-order photon-added superposition.

Funding statement

This research is funded by the Vietnam Ministry of Education and Training (MOET) under grant number B2019-DHH-12.

References

1. Aasi J, Abadie J, Abbott BP, Abbott R, Abbott TD, Abernathy MR, et al. Enhanced sensitivity of the LIGO gravitational wave detector by using squeezed states of light. *Nature Photonics*. *Nature Photonics*. 2013;7(8):613-619.
2. Pathak A, Garcia ME. Control of higher-order antibunching. *Applied Physics B*. 2006;84:479-484.
3. Bennett CH, Brassard G, Crépeau C, Jozsa R, Peres A, Wootters WK. Teleporting an unknown quantum state via dual classic and Einstein-Podolsky-Rosen channels. *Physical Review Letters*. 1993;70:1895-1899.
4. Hillery M, Berthiaume A. Quantum Secret Sharing. *Physical Review A*. 1999;59:1829-1834.
5. Hong L, Guo GC. Non-classical properties of photon-added pair coherent states. *Acta Physica Sinica (Overseas Edition)*. 1999;8(8):577-582.
6. Truong DM, Nguyen HTX, Nguyen AB. Sum Squeezing, Difference Squeezing, Higher-Order Antibunching and Entanglement of Two-Mode Photon-Added Displaced Squeezed States. *International Journal of Theoretical Physics*. 2013;53(3):899-910.
7. Wang S, Hou LL, Chen XF, Xu XF. Continuous-variable quantum teleportation with non-Gaussian entangled states generated via multiple-photon subtraction and addition. *Physical Review A*. 2015;91:063832.
8. Duc TM, Dinh DH, Dat TQ. Higher-order non-classical properties of nonlinear charge pair cat states. *Journal of Physics B: Atomic, Molecular and Optical Physics*. 2020;53:025402.
9. Agarwal GS, Tara K. Non-classical properties of states generated by the excitations on a coherent state. *Physical Review A*. 1991;43:492.
10. Duc TM, Noh J. Higher-order properties of photon-added coherent states. *Optics Communications*. 2008;281:2842.
11. An NB, Duc TM. Excited K-quantum nonlinear coherent states. *Journal of Physics A: Mathematical and General*. 2002;35:4749.
12. Duc TM, Dat TQ. Enhancing nonclassical and entanglement properties of trio coherent states by photon-addition. *Optik*. 2020;210:164479.
13. Wang XB, Kwek LC, Liu Y, Oh CH. Non-classical effects of two-mode photon-added displaced squeezed states. *Journal of Physics B: Atomic, Molecular and Optical Physics*. 2001;34:1059.
14. Hu LY, Zhang ZM. Non-classicality and decoherence of photon-added squeezed thermal state

- in thermal environment. *Journal of the Optical Society of America B*. 2012;29:529.
15. Duc TM, Dat TQ, Chuong HS. Quantum entanglement and teleportation in superposition of multiple-photon-added two-mode squeezed vacuum state. *International Journal of Modern Physics B*. 2020;34(25):2050223.
 16. Lee CT. Simple criterion for non-classical two-mode states. *Journal of the Optical Society of America B*. 1998;15:1187.
 17. Dat TQ, Duc TM. Higher-order non-classical and entanglement properties in photon-added trio coherent state. *Hue University Journal of Science: Natural Science*. 2020;129(1B):49-55.
 18. Fiurasek J. Conditional generation of N-photon entangled states of light. *Physical Review A*. 2002;65:053818.
 19. Lee SY, Nha H. Second-order superposition operations via Hong-Ou-Mandel interference. *Physical Review A*. 2012;85:043816.
 20. Dat TQ, Duc TM. Non-classical properties of the superposition of three-mode photon-added trio coherent state. *International Journal of Theoretical Physics*. 2020;59:3206-3216.
 21. Caves CM, Schumaker BL. New formalism for two-photon quantum optics. I. Quadrature phases and squeezed states. *Physical Review A*. 1985;31:3068.
 22. Braunstein SL, van Loock P. Quantum information with continuous variables. *Reviews of Modern Physics*. 2005;77(2):513-577.
 23. Furusawa A, Sorensen JL, Braunstein SL, Fuchs CA, Kimble HJ, Polzik ES. Unconditional quantum teleportation. *Science*. 1998;282:706.
 24. Hoai NTX, Duc TM. Nonclassical properties and teleportation in the two-mode photon-added displaced squeezed states. *International Journal of Modern Physics B*. 2016;30(7):1650032.
 25. Kenfack A, Zyczkowski K. Negativity of the Wigner function as an indicator of non-classicality. *Journal of Optics B: Quantum and Semiclassical Optics*. 2004;6:396.
 26. Clark JB, Lecocq F, Simmonds RW, Aumentado J, Teufel JD. Sideband cooling beyond the quantum back action limit with squeezed light. *Nature*. 2017;541:191.
 27. Hillery M. Sum and difference squeezing of the electromagnetic field. *Physical Review A*. 1989;40:3147.